



Enhancing the thermal conductivity of ethylene-vinyl acetate (EVA) in a photovoltaic thermal collector

J. Allan, H. Pinder, and Z. Dehouche

Citation: *AIP Advances* **6**, 035011 (2016); doi: 10.1063/1.4944557

View online: <http://dx.doi.org/10.1063/1.4944557>

View Table of Contents: <http://scitation.aip.org/content/aip/journal/adva/6/3?ver=pdfcov>

Published by the *AIP Publishing*

Articles you may be interested in

[Prestrain relaxation in non-covalently modified ethylene-vinyl acetate | PyChol | multiwall carbon nanotube nanocomposites](#)

APL Mater. **2**, 066105 (2014); 10.1063/1.4884216

[Study on thermal properties and crystallization behavior of electron beam irradiated ethylene vinyl acetate \(EVA\)/waste tyre dust \(WTD\) blends in the presence of polyethylene graft maleic anhydride \(PEgMAH\)](#)

AIP Conf. Proc. **1571**, 146 (2013); 10.1063/1.4858645

[Diffusion of mineral oils in ethylene-vinyl acetate copolymer](#)

AIP Conf. Proc. **1459**, 42 (2012); 10.1063/1.4738392

[Ethylene-vinyl Alcohol Copolymer \(EvOH\) by XPS](#)

Surf. Sci. Spectra **6**, 137 (1999); 10.1116/1.1247918

[Thermally stimulated currents in polyethylene and ethylene–vinyl-acetate copolymers](#)

J. Appl. Phys. **48**, 2408 (1977); 10.1063/1.324003

The cover image for AIP Applied Physics Reviews, featuring a blue and orange color scheme with a molecular structure background. The text 'NEW Special Topic Sections' is prominently displayed in white. Below it, the text 'NOW ONLINE Lithium Niobate Properties and Applications: Reviews of Emerging Trends' is shown in orange and white. The AIP Applied Physics Reviews logo is in the bottom right corner.

NEW Special Topic Sections

NOW ONLINE
Lithium Niobate Properties and Applications:
Reviews of Emerging Trends

AIP Applied Physics Reviews

Enhancing the thermal conductivity of ethylene-vinyl acetate (EVA) in a photovoltaic thermal collector

J. Allan,^{1,2,a} H. Pinder,¹ and Z. Dehouche¹

¹School of Engineering and Design, Brunel University, London, UB8 3PH, United Kingdom

²ChapmanBDSP, Saffron House, 6-10 Kirby Street, London, EC1N 8EQ, United Kingdom

(Received 7 November 2015; accepted 1 March 2016; published online 15 March 2016)

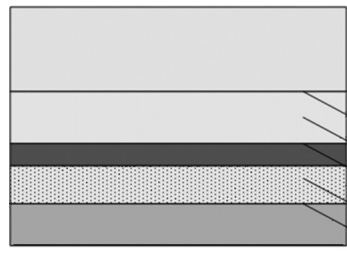
Samples of Ethylene-Vinyl Acetate (EVA) were doped with particles of Boron Nitride (BN) in concentrations ranging from 0-60% w/w. Thermal conductivity was measured using a Differential Scanning Calorimetry (DSC) technique. The thermal conductivity of parent EVA was increased from 0.24W/m·K to 0.80W/m·K for the 60% w/w sample. Two PV laminates were made; one using the parent EVA the other using EVA doped with 50% BN. When exposed to a one directional heat flux the doped laminate was, on average, 6% cooler than the standard laminate. A finite difference model had good agreement with experimental results and showed that the use of 60% BN composite achieved a PV performance increase of 0.3% compared to the standard laminate. © 2016 Author(s). All article content, except where otherwise noted, is licensed under a Creative Commons Attribution 3.0 Unported License. [<http://dx.doi.org/10.1063/1.4944557>]

NOMENCLATURE

A	Area [m ²]
D	Disc Thickness [m]
g	Volumetric heat generation [W/m ³]
h	Convective heat transfer coefficient W/m ² ·K
k	Thermal conductivity [W/m·K]
K_{eb}	Thermal conductivity of back EVA layer [W/m·K]
K_{ef}	Thermal conductivity of front EVA layer [W/m·K]
K_g	Thermal conductivity of glass [W/m·K]
K_{pv}	Thermal conductivity of PV cell [W/m·K]
K_t	Thermal conductivity of tedlar [W/m·K]
M	Gradient of slope
T	Temperature [K]
V	Volume [m ³]
W	Weight [kg]
x_{eb}	Thickness of back EVA layer [m]
x_{ef}	Thickness of front EVA layer [m]
x_g	Thickness of glass layer [m]
x_{pv}	Thickness of PV layer [m]
x_t	Thickness of tedlar layer [m]
δ	Thickness [m]
α_g	Thermal diffusivity of PV layer [m ² /s]
α_{pv}	Thermal diffusivity of glass layer [m ² /s]
λ	Thermal Conductivity [W/m·K]
ϕ	Volume fraction

^aCorresponding author james.p.allan14@gmail.com





Layer	Layer Thickness (m)	Thermal Conductivity (W/m ² ·K)
Glass	0.003	0.98
EVA	0.0004	0.23
Solar Cell	0.00018	148
EVA	0.0004	0.23
Tedlar	0.0005	0.36

FIG. 1. The layers of a PV laminate and their respective thicknesses and thermal conductivities. Thickness and thermal conductivity from Ref. 3.

BACKGROUND

As the temperature of a PV cell increases, its electrical efficiency decreases. Estimates of the annual losses in performance due to temperature vary from 2.2 to 17.5%.¹ This loss is influenced by installation method; it has been shown that free-standing and ground mounted systems experience less temperature losses than those that are building integrated.²

EVA is used to encapsulate PV cells and prevent environmental degradation; however these materials have low thermal conductivity. The multiple layers found in a typical PV laminate are shown in Figure 1.

The composite conductivity through the collector can be calculated using (1.1).

$$k_{total} = \frac{\delta_{total}}{\frac{\delta_{eva}}{k_{eva}} + \frac{\delta_{si}}{k_{si}} + \frac{\delta_{ted}}{k_{ted}} + \frac{\delta_{alu}}{k_{alu}}} \quad (1.1)$$

Using the values in Figure 1, the calculated conductivity of the composite is 0.82W/(m·K). If the conductivity of the EVA layer on the backside of the PV cell is increased from 0.23W/(m·K) to 2.85W/(m·K),³ the overall composite conductivity increases by nearly 25% to 1.02W/(m·K).

Enhancing the Thermal Conductivity of EVA

EVA can be mixed with other materials to form composites with intrinsically different properties to the parent material. The mixing of ceramic powders and polymers, to increase thermal conductivity, is used in microelectronics, where heat needs to be efficiently dissipated away from sensitive chips and processors.⁴

The same concept can be applied to photovoltaic cells. A previous study by Lee *et al.*³ revealed that filler materials increase the thermal conductivity of EVA from 0.23 to 2.85W/(m·K). For a range of different filler materials, a concentration of 20% v/v resulted in a -0.97% to +5.05% change in power output compared to the parent material.. Kemaloglu *et al.*⁵ used Boron Nitride filler with a particle size of approximately 10μm; the conclusion was that conductivity increases with reduced particle size and that nano-sized particles hold promise for the future.

Measuring Thermal Conductivity

Thermal conductivity can be measured using the method outlined in ASTM E1952.⁶ This method uses modulated differential scanning calorimetry (mDSC) to determine the specific heat capacity, which is then used to calculate the thermal conductivity. Thermal conductivity can also be measured using DSC by placing a ‘melting standard’ on top of the specimen.⁷ When heat is supplied from the DSC furnace, the specimen’s conductivity is proportional to the melting rate of the standard and can be quantified through comparison with a reference material. The method was developed using metals such as gallium and indium as the melting reference material and has since been applied to a number of other materials.⁸⁻¹¹



FIG. 2. Twin screw extrusion of the composite material.

METHODOLOGY

Sample Preparation

BN powder (Carbotherm, Saint-Gobain, France) was mixed with EVA granules, in concentrations ranging from 10-60% w/w, using twin screw extrusion (HAAKE MiniLab II, Thermo Scientific, US) see Figure 2. The resulting extrusions were compression molded, to form sheets with a thickness of 1 mm.

Measuring Thermal Conductivity

6 mm discs were punched from the compressed sheets and placed into a DSC sample pan. The thermal interface resistance between the pan and the sample was reduced using a thin film of silicone oil, applied directly to the underside of the sample. Crodatherm-25 phase change material (PCM) (Croda, UK) was used as the melting standard because its melting point (25°C) is well below that of EVA (89°C). The thermophysical properties of Crodatherm are provided in Table III of the Appendix. Approximately 2mg of the PCM melting standard was deposited on the surface of the sample disc. This was achieved by gently heating the PCM material above its melting point in a glass pipette, before releasing it and allowing it to recrystallise on the surface of the sample. The method assumes unidirectional heat flow from the DSC furnace, through the sample and into the melting standard. Care had to be taken to ensure that there was no contact between the aluminum pan and the melting standard. The sample pan was then placed, un-crimped, into the sample chamber of the DSC (Perkin Elmer, US), the DSC process is illustrated in Figure 3. The sample was cooled to -10°C before being heated to 40°C at 5°C/min. The graph of heat flux vs. temperature, produced by the DSC was analyzed to determine melting rate of the sample. Low Density Polyethylene

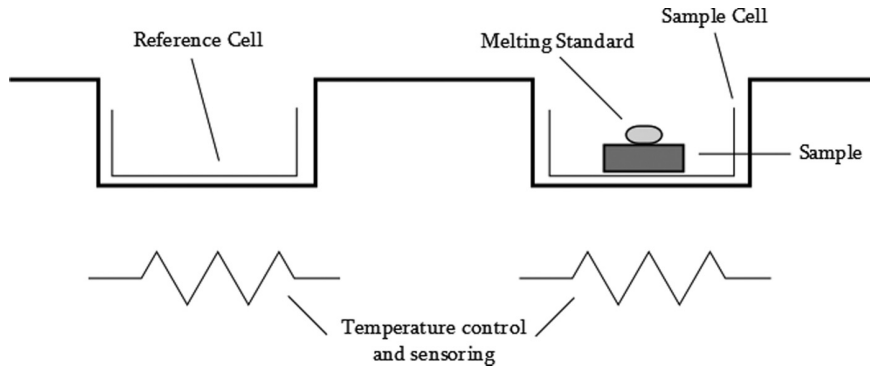


FIG. 3. Illustration of the DSC melting standard method.

(LDPE) with a certified conductivity of 0.33W/m·K (Goodfellow Cambridge Ltd., UK) was used as the reference material and was prepared using the same method detailed above.

The melting rate is then calculated as the gradient of a line connecting the melting onset and melting point, see Figure 4. Equation (1.2) is then used to determine the thermal conductivity of the sample.⁹

$$\lambda_s = \lambda_r \frac{D_s A_r}{D_r A_s} \left(\frac{M_s}{M_r} \right)^2 \quad (1.2)$$

Where the subscripts r and s denote reference and sample respectively, D is disc thickness, A is the disc area, M is the melting rate and λ is the thermal conductivity.

Manufacture of PV laminate

The parent EVA material and doped extrusions were compression molded into 0.5 mm thick sheets measuring 155mm x 155mm. Two cells were laminated independently; one using the parent EVA, the other using the 50% BN/EVA w/w composite.

0.12 mm T-type thermocouples (Omega, US) were positioned between the layers shown in Figure 1. The laminate was then placed between a constant heat source (25W ceramic heating mat) and heat sink (chilled absorber plate with inlet set to 21°C) to generate a one directional heat flux through the laminate. The thermocouples recorded the temperature at each layer as the heat flux passed through the laminate.

Numerical Models

A numerical model based on the finite difference approach was developed to simulate the temperature distribution across the cross section of the PV laminate. The finite difference approach is shown in Figure 5.

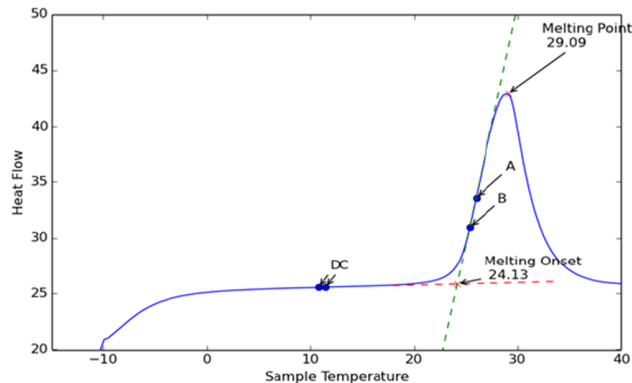


FIG. 4. Melting curve of Crodatherm PCM.

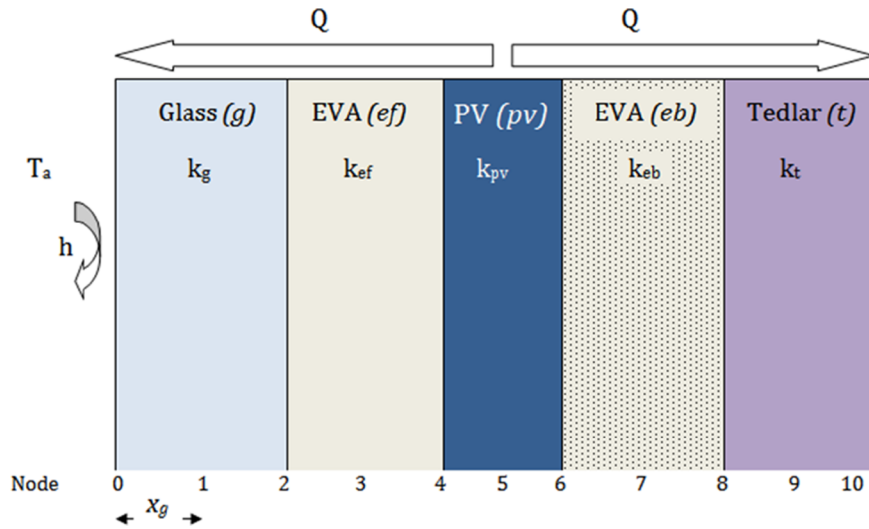


FIG. 5. Illustration of the finite difference model applied to a PV laminate.

A system of equations was created to represent the PV laminate shown in Figure 5. A different equation was required for each nodal type. The four nodal types in this model are; exterior interface, layer node, internal interface and heat generation layer. An example of the equations for each type is provided in Table I. The problem was solved iteratively using a program coded in Fortran and the code is supplied in the [Appendix](#).

RESULTS

Thermal Conductivity

EVA:BN composite was prepared with varying concentration of BN filler (10,20,30 and 60%) weight %. The thermal conductivity was measured for each sample and the results are shown in Figure 6.

Figure 6 shows that, by increasing the BN concentration from 0% to 60% w/w, thermal conductivity increases from 0.23 W/m·K to 0.83 W/m·K, with a linear regression value of 0.9956. To compare the results with the findings of the study by Lee³ the mass fraction must be converted to volume fraction, φ , using (1.3).

$$V = \frac{W_E}{\rho_E} + \frac{W_B}{\rho_B} = V_E + V_B \quad (1.3)$$

$$\varphi_B = \frac{V_B}{V}$$

TABLE I. Example of the equations used to represent the heat transfer through the laminate cross section.

Nodal Type	Example node	Temperature at example node
Exterior Interface	0	$T_0 = \frac{hT_a + \left(\frac{1}{x_g} k_g T_1\right)}{h + \left(\frac{1}{x_g} k_g\right)}$
Layer Node	1	$T_1 = (T_0 + T_2) / 2$
Internal Interface	4	$T_4 = \frac{k_{ef} \frac{1}{x_{ef}} (T_3) + k_{pv} \frac{1}{x_{pv}} (T_5) + \dot{q}_{pv} \left(\frac{x_{pv}}{2}\right)}{k_{ef} \frac{1}{x_{ef}} + k_{pv} \frac{1}{x_{pv}}}$
Heat Generating PV Layer	5	$T_5 = \frac{\frac{1}{x_{pv}} (T_4) + \frac{1}{x_{pv}} (T_6) + \frac{\dot{q}_{pv}}{k_{pv}}}{2 \left(\frac{1}{x_{pv}}\right)}$

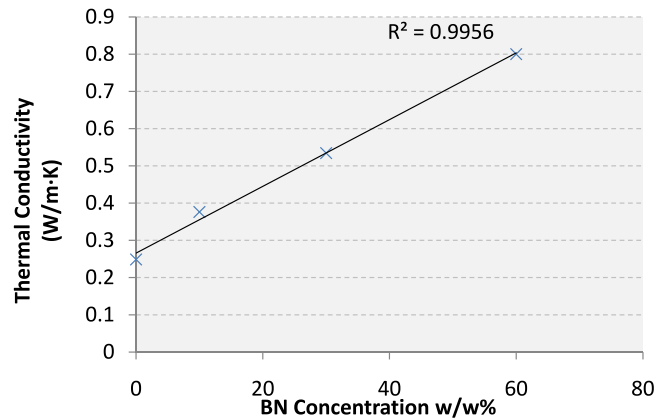


FIG. 6. Thermal conductivity vs. boron nitride concentration.

Where W , V and ρ are the weight, volume and density respectively; and subscripts, E and B denote EVA and BN respectively.

For 60% w/w Boron Nitride to EVA, the corresponding volume fraction is approximately 40% v/v as shown in Table II. For 40% v/v BN concentration Lee *et al.* reported a thermal conductivity of approximately $0.75 \text{ W/m}\cdot\text{K}^3$ which is agreement with the $0.83 \text{ W/m}\cdot\text{K}$ measured in this study. Lee *et al.* continued to increase the BN concentration up to 60% v/v; however it was found that increased filler increased the stiffness of the material, which could cause problems for manufacture and durability. The same issue was experienced in this study.

Interface Temperature

The thermocouples did not embed seamlessly between the layers; instead air bubbles formed around each thermocouple. An attempt was made to reduce the thickness of the thermocouple wire to 0.12 mm; however air bubbles were still present. To compensate for this variation, an average laminate temperature was calculated. A comparison of the doped vs standard EVA case is shown in Figure 7. The doped laminate was consistently around 6% cooler than the standard laminate, under the same conditions.

Numerical Models

The temperature profile across the external, interior and interface nodes were plotted for two cases and three conductivities of backing-EVA. In Case 1 the rear surface temperature of the laminate, T10, was fixed at a 25°C . This case resembles the temperature controlled absorber plate of a PVT collector. The top surface was assigned an overall loss coefficient of $11 \text{ W/m}^2\cdot^\circ\text{C}$

In Case 1, shown in Figure 8, the temperature of the PV cell, T5, is highest for the un-doped EVA. As the thermal conductivity of the backing-EVA increases, the PV cell temperature reduces. A temperature reduction of 0.7°C in PV cell temperature is seen when thermal conductivity of the backing-EVA is increased from $0.23 \text{ W/m}\cdot\text{K}$ to $0.83 \text{ W/m}\cdot\text{K}$. Using the power temperature coefficient for a crystalline cell, as supplied by the manufacturer ($-0.42\%/K$), this would enhance the performance by 0.3%. Further increasing the thermal conductivity to $2.85 \text{ W/m}\cdot\text{K}$, the PV cell temperature is reduced by an additional 0.2°C indicating a non-linear relationship between the

TABLE II. Calculation of volume fraction.

	Weight [%]	Density (g/cm^3)	Volume [cm^3]	Volume Fraction
EVA	40	0.935^{12}	42.78	62.1%
Boron Nitride	60	2.3^{13}	26.09	37.9%

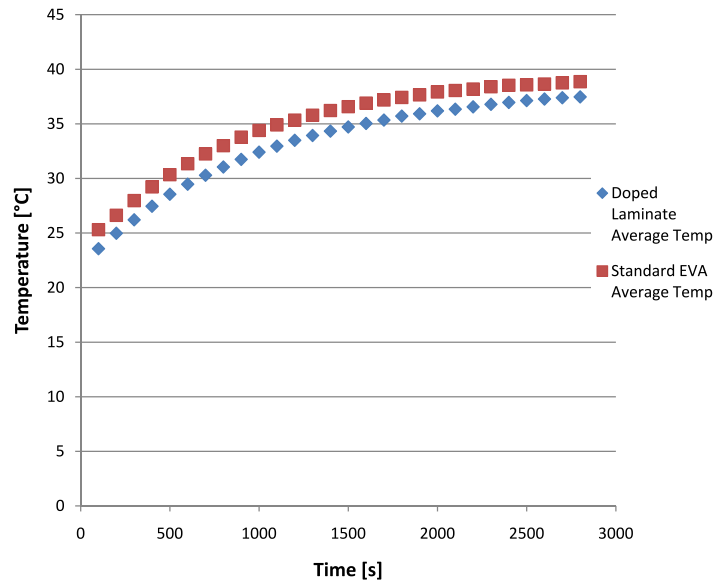


FIG. 7. A comparison of the average laminate temperature for the enhanced and standard material.

conductivity of the backing-EVA and PV cell temperature. The increased conductivity of the backing encapsulant also reduces the overall temperature of the laminate. The front surface of the panel is hottest for the $0.23\text{W/m}\cdot\text{K}$ and coldest for the $2.85\text{W/m}\cdot\text{K}$ backing-EVA.

In Case 2, a heat loss coefficient was applied to both the top surface and the rear surface of the laminate; resembling a PV module that is evenly ventilated on each surface. The ambient temperature was kept at 20°C .

In Case 2, shown in Figure 9, the temperature of the PV cell highest for the standard EVA; however, when the thermal conductivity is increased from $0.23\text{W/m}\cdot\text{K}$ to $0.83\text{W/m}\cdot\text{K}$, the temperature difference is much smaller than Case 1 at 0.1°C , equating to a power improvement of 0.04% . The temperature difference between $0.83\text{W/m}\cdot\text{K}$ and $2.85\text{W/m}\cdot\text{K}$ is negligible. The rear surface temperature, T10, is lowest for the $0.23\text{W/m}\cdot\text{K}$ backing-EVA and highest for the $2.85\text{W/m}\cdot\text{K}$. This is due to the low thermal conductivity of the backing material reducing heat flow and insulating the PV cell. This results in a higher PV cell temperature and lower surface temperature.

The PV cell temperature for Case 2 is higher (49.6°C) than that of Case 1 (26.7°C); which is a 10% improvement in power output from the PV cell; thus showing the ability of a PVT collector to maintain the operating efficiency of the PV cell.

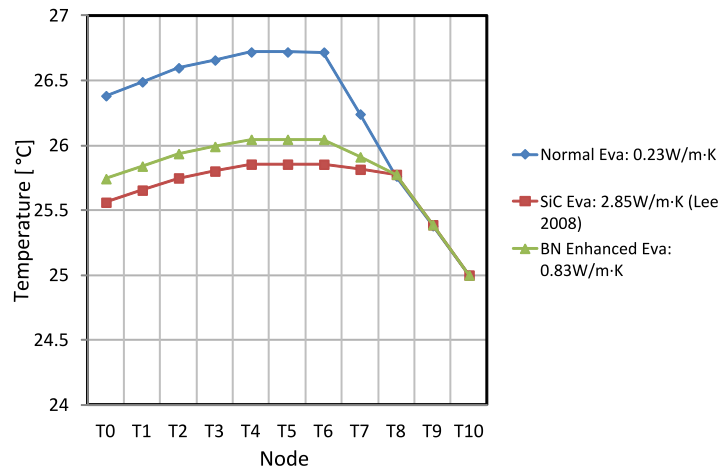


FIG. 8. Temperature profile for Case 1; PV laminate in contact with PVT absorber.

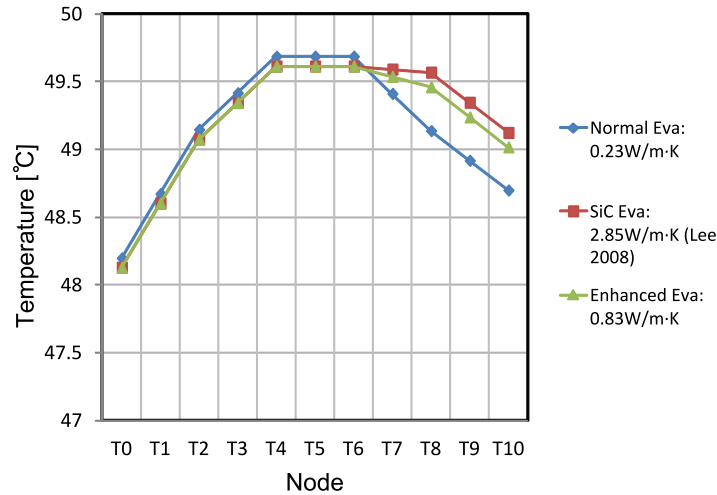


FIG. 9. Temperature profile for Case 2; naturally ventilated PV laminate.

The Carbotherm filler costs 240€/kg; it is believed that the improvements in both Case 1 and 2 do not justify the additional material and manufacturing costs.

CONCLUSION

Doping EVA with boron nitride increased the thermal conductivity by a factor of 4; which is in agreement with previous studies. However it was noticed that the material became stiffer and more brittle with increasing filler content. Further work is required to determine how this will influence the manufacture and lifetime of the PV module. A numerical model showed improvement in performance was 0.3% for a PVT collector. Considering the high price of thermal fillers, further research should focus on whether they are worth the cost for such a small increase in performance. Perhaps their use would be more suited to concentrator systems where higher temperatures are experienced.

ACKNOWLEDGEMENTS

This work was sponsored by ChapmanBDSP, London, UK and the Engineering and Physical Research Council, UK.

APPENDIX

TABLE III. Thermophysical properties of CrodaTherm 25, as provided by the manufacturer.

Test	Typical Value	Units
Melting Temperature	25	°C
Latent Heat, Melting	186	kJ/kg
Crystallisation temperature	22	°C
Latent Heat, Crystallisation	-184	kJ/kg
Volumetric Heat Capacity	170	C(mJ/m ³)
Specific Heat Capacity, Solid	1.9	kJ/(kg·°C)
Specific Heat Capacity, Liquid	2.3	kJ/(kg·°C)
Thermal conductivity, solid	0.21	W/(m·°C)
Thermal conductivity, liquid	0.15	W/(m·°C)

Fortran Program for finite difference analysis

PROGRAM STEADY

DATA T0,T1,T2,T3,T4,T5,T6,T7,T8,T10/10*50/

DATA T9/50/

!Boundary Temperatures and heat loss coefficient

real,parameter::Tp=25., Ta=20., h=11.,Tb=20., hb=11.

!Material Conductivity

real,parameter:: kg=0.98, kef=0.23, kpv=148., keb=2.85, kt=0.36

!Nodal Spacing

real,parameter:: xg=0.0015, xef=0.0002, xpv=0.00009, xeb=0.0002, xt=0.00025

!Volumetric Energy Generation

real,parameter:: gpv=3.46E6

!Results file

integer, parameter :: out_unit=20

OPEN (unit=out_unit,file="results.txt",action="write",status="replace")

DO 20 K=1,500000

T10=((h*tb)+((1/xt)*(kt)*(T9)))/(h+((1/xt)*(kt)))

T9=(T8+T10)/2.

T8(((1./xeb)*keb*t7)+((1./xt)*kt*t9))/(keb*(1./xeb)+(kt*(1./xt)))

T7=(T6+T8)/2.

T6(((1./xpv)*kpvt5)+((1./xeb)*keb*t7)+(gpv*(xpv/2.)))/((kpvt(1./xpv)+(keb*(1./xeb)))

T5(((1./xpv2)*t4)+((1./xpv**2)*t6)+(gpv/kpv))/(2.*(1./xpv**2))**

T4(((1./xef)*keft3)+((1./xpv)*kpvt5)+(gpv*(xpv/2.)))/((keft(1./xef)+(kpvt(1./xpv)))

T3=(T2+T4)/2.

T2(((1./xg)*kgt1)+((1./xef)*keft3))/(kgt(1./xg)+(keft(1./xef)))

T1=(T0+T2)/2.

T0=((h*ta)+((1./xg)*(kg)*(T1)))/(h+((1./xg)*(kg)))

WRITE (*,10)K,T0,T1,T2,T3,T4,T5,T6,T7,T8,T9

if (mod(k,1000)==0) WRITE

(out_unit,*K, ",",T0, ",",T1, ",",T2, ",",T3, ",",T4, ",",T5, ",",T6, ",",T7, ",",T8, ",",T9, ",",T10

10 FORMAT (' ',I3,10(F8.1))

20 CONTINUE

END PROGRAM STEADY

- ¹ Brian Norton, Philip C Eames, Tapas K Mallick, Ming Jun Huang, Sarah J McCormack, Jayanta D Mondol, and Yigzaw G Yohanis, "Enhancing the performance of building integrated photovoltaics," *Solar Energy* **85**(8), 1629–1664 (2011).
- ² T. Nordmann and L. Clavadetscher, "Understanding temperature effects on pv system performance," in *Photovoltaic Energy Conversion, 2003. Proceedings of 3rd World Conference on* (IEEE, 2003), Vol. 3, pp. 2243–2246.
- ³ B Lee, JZ Liu, Bin Sun, CY Shen, and GC Dai, "Thermally conductive and electrically insulating eva composite encapsulants for solar photovoltaic (pv) cell," *eXPRESS Polymer Letters* **2**(5), 357–363 (2008).
- ⁴ Geon-Woong Lee, Min Park, Junkyung Kim, Jae Ik Lee, and Ho Gyu Yoon, "Enhanced thermal conductivity of polymer composites filled with hybrid filler," *Composites Part A: Applied Science and Manufacturing* **37**(5), 727–734 (2006).
- ⁵ Sebnem Kemalglu, Guralp Ozkoc, and Ayse Aytac, "Thermally conductive boron nitride/sebs/eva ternary composites: "processing and characterization"?, *Polymer Composites* **31**(8), 1398–1408 (2010).
- ⁶ ASTM, "Standard test method for thermal conductivity and thermal diffusivity by modulated temperature differential scanning calorimetry," Technical report (ASTM Internation, (2006).
- ⁷ G Hakvoort, LL Van Reijen, and AJ Aartsen, "Measurement of the thermal conductivity of solid substances by dsc," *Thermochemica acta* **93**, 317–320 (1985).
- ⁸ Joseph H Flynn and David M Levin, "A method for the determination of thermal conductivity of sheet materials by differential scanning calorimetry (dsc)," *Thermochemica acta* **126**, 93–100 (1988).
- ⁹ Z Dehouche, N Grimard, F Laurencelle, J Goyette, and TK Bose, "Hydride alloys properties investigations for hydrogen sorption compressor," *Journal of Alloys and compounds* **399**(1), 224–236 (2005).
- ¹⁰ H Fukushima, LT Drzal, BP Rook, and MJ Rich, "Thermal conductivity of exfoliated graphite nanocomposites," *Journal of thermal analysis and calorimetry* **85**(1), 235–238 (2006).
- ¹¹ Duncan M Price and Mark Jarratt, "Thermal conductivity of ptfe and ptfe composites," *Thermochemica acta* **392**, 231–236 (2002).
- ¹² Total. Ethylene vinyl acetate copolymers (eva) (2014).
- ¹³ Azom. Boron nitride (bn) - properties and information on boron nitride.